Journal of Hazardous Materials 185 (2011) 117–123

Contents lists available at ScienceDirect

Journal of Hazardous Materials

journal homepage: www.elsevier.com/locate/jhazmat

Efficient photodegradation of dyes using light-induced self assembly TiO_2/β-cyclodextrin hybrid nanoparticles under visible light irradiation

Xu Zhang, Feng Wu, Nansheng Deng*

School of Resources and Environmental Science, Hubei Key Laboratory of Biomass-Resources, Wuhan University, Wuhan 430079, PR China

ARTICLE INFO

Article history:
Received 22 May 2010
Received in revised form 28 August 2010
Accepted 1 September 2010
Available online 15 September 2010

Keywords:
β-cyclodextrin
Self assembly
Superoxide radical
TiO_2

ABSTRACT

A novel β-cyclodextrin (β-CD) grafted titanium dioxide (TiO_2/β-CD) was synthesized through photo-induced self assembly methods, and its structure was characterized. The TiO_2/β-CD hybrid nanomaterial showed high photoactivity under visible light irradiation ($\lambda \geq 400$ nm and/or $\lambda \geq 420$ nm) and simulated solar irradiation ($\lambda \geq 365$ nm). Photodegradation of Orange II followed the Langmuir–Hinshelwood kinetics model. The initial rate R_0 of Orange II degradation increased by 6.9, 2.6 and 1.9 times in the irradiation conditions of $\lambda \geq 420$ nm, $\lambda \geq 400$ nm and $\lambda \geq 365$ nm, respectively. β-CD increased the lifetimes of the excited states of the unreactive guests and facilitated the electron transfer from the excited dye to the TiO_2 conduction band, which enhanced the dye pollutant degradation. Superoxide radicals were shown to be the main reactive species that caused the degradation of Orange II under visible irradiation.

1. Introduction

In recent decades, titanium dioxide (TiO_2) has been applied in many areas since Fujishima and Honda first discovered photochemical water splitting by a chemically modified n-TiO_2 electrode [1]. There has also been an increased interest in using TiO_2 as a catalyst in the environmental realm. The photocatalytic degradation of various organic pollutants, the photo-reduction of inorganic contaminantes and the inactivation of microorganisms have been performed with noteworthy results [2–5]. Most organic pollutants can be completely decomposed into carbon dioxide and water when TiO_2 is used as the photocatalyst, mainly because the photogenerated holes and hydroxyl radicals are the most powerful oxidants. However, TiO_2 can only use less than 5% of the available due to its large band gap (3.2 eV). Furthermore, the high electron-hole recombination rate also makes it a relatively inefficient photocatalyst. Successful improvement of TiO_2 performance requires the lowering of the band gap to use visible light and restricting the charge-hole recombination to enhance quantum efficiency.

Synthetic dyes are manufactured and used for numerous industrial applications, such as textiles, leather goods, food manufacturing and other chemical uses. It is estimated that, out of the total amount of dyes in use, 1–2% in manufacturing and 1–10% are released into water, air and soil [6]. Dye pollutants can be bleach under visible irradiation through photosensitized degradation on a semiconductor surface. However, only an adsorbed dye molecule can inject the charge from its excited state to the semiconductor's conduction band. Thus, the degradation is usually inefficient.

Cyclodextrin (CD) modified TiO_2 has attracted rnewed interest since Willner and colleagues observed that β-CD could stabilize TiO_2 colloids and facilitate interfacial electron transfer processes [7–9]. Excellent literature has been published to elucidate the effect of β-CD on TiO_2 photochemical properties [10–14]. All previous work suggests that β-CD plays electron-donating and hole-capturing roles when linked to TiO_2 colloids, which lead to charge-hole recombination restriction and photocatalytic efficiency enhancement. Some previous papers have reported the stimulative effect of cyclodextrin on the photocatalytic degradation of organic pollutants in TiO_2 suspensions [15–18]. However, it is difficult to recover cyclodextrin after the reaction because β-CD is an expensive reagent. Furthermore, synthesizing β-CD modified TiO_2 colloids is complicated and time-consuming, and the colloids were only stable in acidic conditions. Therefore, it is worthwhile to synthesize a β-CD grafted TiO_2 hybrid powder using a new method and investigate its catalytic performance.

Recently, Toma et al. synthesized carboxymethyl-β-cyclodextrin modified mesoporous TiO_2 films by immersing TiO_2 films in carboxymethyl-β-cyclodextrin solution [19]. Feng et al. reported that CDs could irreversibly coat the surface of anatase TiO_2 particles under UV irradiation to form wire-like composites [13]. In addition, Zhou et al reported the solar-induced self-assembly of TiO_2–β-cyclodextrin–MWCNT composite wires

* Corresponding author. Tel.: +86 27 68778511; fax: +86 27 68778511.
E-mail address: nsdeng@gmail.com (N. Deng).

0304-3894/$ – see front matter © 2010 Elsevier B.V. All rights reserved.
doi:10.1016/j.jhazmat.2010.09.005

[20]. However, there are few reports about the photoactivity of the hybrid nanomaterials.

TiO_2/β-CD hybrid nanoparticles were synthesized by a photo-induced self assembly process in this work. The photoactivity of the TiO_2/β-CD hybrid nanoparticles under visible light irradiation ($\lambda \geq 400$ nm and/or $\lambda \geq 420$ nm) and simulated solar irradiation ($\lambda \geq 365$ nm, with a metal halide lamp) was investigated. β-CD is hypothesized to play a role as a "channel" or "bridge" between the dyes and TiO_2 powders, which facilitates the electron injection from excited dyes to the conduction band of TiO_2.

2. Materials and methods

2.1. Chemicals

β-CD was purchased from Wako Pure Chemical Inc. (≥97%). Anatase TiO_2 was purchased from High Technology Nano Co. Ltd. (Nanjing, China). Degussa P25 from Degussa AG-Germany. Orange II was purchased from Shang Hai SSS Regent Co., LTD and used as the model dye pollutants. 1,4-Benzoquinone and *tert*-butyl alcohol (*t*-BuOH) were used as the superoxide radical quencher and the hydroxyl radical scavenger, respectively. Sodium azide was used as a scavenger of singlet oxygen and hydroxyl radicals. All scavengers were purchased from Shanghai Reagent Co Ltd. (Shanghai, China). Milli-Q deionized water (18.2 MΩ cm) was used as the solvent. All other reagents were analytical grade and used as received.

2.2. Preparation of TiO_2/β-CD

In a typical synthesis of TiO_2/β-CD hybrid nanoparticles, a 2.0 g L^{-1} anatase TiO_2 and 10.0 g L^{-1} β-CD suspended solution was irradiated under a 15 W UV disinfection lamp (Xinghui Lamp Co. Ltd, Hunan, PRC, emitting 254 nm light with an intensity of 1.04×10^{-5} Ein L^{-1} s^{-1}), as established by ferrioxalate actinometry for 24 h with continuous air bubbling [21]. The suspension was centrifuged and the solid phase was collected and redispersed in a fresh 10.0 g L^{-1} β-CD solution, which was irradiated for another 24 h. The suspended solution was centrifuged, and the solid phase was carefully washed with ultrapure water until no β-CD was detected in the supernatant liquid by phenolphthalein colorimetry. The TiO_2/β-CD hybrid nanoparticles were dried under dynamic vacuum for 12 h at 50 °C. Although the hybrid catalyst synthesized from previous method [22] showed slightly higher activity than that of the material synthesized in this work (Fig. S1 of Supporting Information), the method in this work is more convenient. Reference material was synthesized using the same procedures but omitting cyclodextrin.

2.3. Characterization of TiO_2/β-CD

FT-IR spectra of sample pellets with KBr were recorded on a Fourier transform infrared (FTIR) spectrometer Nicolet 5700 (Thermo Electron Corporation, American). UV–vis diffuse reflectance spectra were recorded on a Shimadzu 2550 UV-vis spectrophotometer with $BaSO_4$ as the background between 200 and 800 nm. The Brunauer-Emmett-Teller surface area was determined using a Gemini V 2380 setup. The XRD patterns of the prepared products were recorded by a Dmax-rA powder diffractometer (Rigaku, Japan), with Cu Kα as a radiation and a step width of 2θ = 0.02°. X-ray photoelectron spectroscopy (XPS) measurements were performed on a XSAM 800 XPS system (Kratos, UK) with a monochromatic Al Kα source. High resolution transmission electron microscopy images were obtained on a JEOL JEM 2010FEF microscope (Japan Electronics, Japan) at an accelerating voltage of 200 kV.

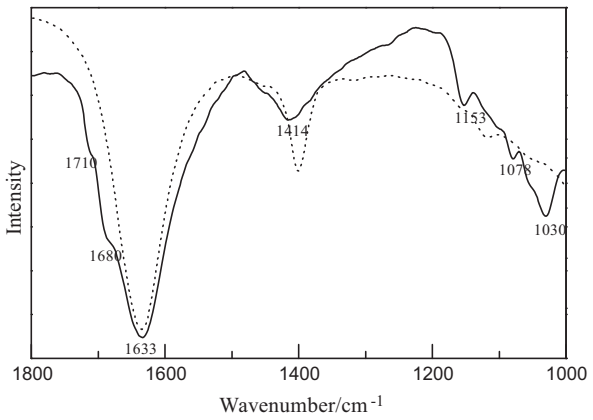

Fig. 1. FT-IR spectra of TiO_2/β-CD hybrid nanoparticle (black line) and TiO_2 (dotted line).

2.4. Photocatalytic degradation

Photodegradation was investigated using a self-made photoreactor [22]. Cutoff filters at 400 and 420 nm (Shimadzu) were used to shield off different wavelengths of light. Orange II aqueous solutions (200 mL) with different catalysts were placed in a 250 mL Pyrex beaker with a magnetic stirrer to mix the solution well. The suspended solution was equilibrated in the dark for half an hour before irradiation. After this period, 5 mL aliquots were withdrawn to determine the concentration C_0. During all oxidation reactions, 5 mL aliquots were collected at selected time intervals, centrifuged and used for concentration determination. The degradation was monitored by a Shimadzu 1601 UV–vis spectrophotometer using a 1 cm cuvette. The initial rate of Orange II photodegradation R_0 (mg L^{-1} h^{-1}) was determined by extrapolating the tangent (based on the linear fit of the points) of the concentration profile back to initial conditions. The total organic carbon (TOC) and total nitrogen (TN) of the solution was measured with an Anlytik Jena AG Multi N/C 2100 TOC/TN instrument. The SO_4^{2-} concentration of was determined by the gravimetric method (with the addition of $BaCl_2$) [23]. Each experiment was performed in triplicates, and all results were expressed as a mean value of the three experiments. Unless otherwise specified, all experiments were carried out at pH 6.0.

3. Results and discussion

3.1. FTIR study

FTIR spectra analysis of TiO_2/β-CD hybrid particles using bare TiO_2 as a reference was investigated in this study (Fig. S2 of Supporting Information). For pure TiO_2, two peaks at 1633.41 and 1397.40 cm^{-1} were assigned to the in-plane bending vibration of the surface OH groups. Fig. 1 shows that the intensity at 1397.40 cm^{-1} decreases and new peaks appear after modification. Peaks centered at 1680 and 1710 cm^{-1} were assigned as the stretching of C=C and C=O bonds, respectively, both of which were not present in pure CD molecules. Absorption at 1414 cm^{-1} was assigned to the O–H in-plane bending, while the antisymmetric C–O–C (glycosidic) stretch was assigned at 1153 cm^{-1}. The absorption at 1078 and 1030 cm^{-1} were both assigned as coupled C–C stretch/C–O stretch vibrations.

3.2. Optical Properties and XRD analysis

Fig. 2 shows the UV-vis DRS spectra of the TiO_2/β-CD nanoparticles using bare TiO_2 as a reference. The Kubelka-Munk formular

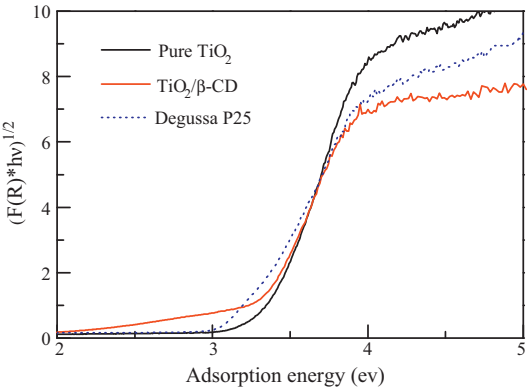

Fig. 2. UV-vis DRS spectra of TiO_2/β-CD hybrid nanoparticle (bold line), TiO_2 (black line) and P25 (dotted line).

was used for all semiconductor samples [24]. CD modification leads to a significant effect on the optical characteristics of anatase TiO_2. The visible absorption intensity of TiO_2/β-CD nanoparticles was much higher than that of bare TiO_2, which is due to the ligand to metal charge transfer (LMCT) between β-CD and Ti^{IV} located in an octahedral coordination environment [10,25]. Although β-CD could also link to the TiO_2 surface without any UV irradiation, the effect on the visible light absorption was smaller [22]. Different synthesis conditions show similar results, and the control material has no absorption features in the visible region and produced a band gap identical to that of pure TiO_2. (Fig. S3 of Supporting Information).

XRD results showed that the anatase TiO_2 conserves its anatase crystal features, and the BET surface area shrinks slightly after the modification (Table S1 of the Supporting Information).

3.3. XPS analysis

XPS analysis was also investigated in this work to attain further information about the surface electronic structure and the chemical valence of bare TiO_2 and TiO_2/β-CD hybrid nanopowders.

The high resolution XPS spectra of the Ti2p region are shown in Fig. 3a. The symmetric shapes of the Ti $2p_{3/2}$ XPS lines indicate that the titanium is present only as Ti^{4+}. The Ti2p region is composed of $2p_{3/2}$ and $2p_{1/2}$ peaks with binding energies (BE) at 458.8 eV and 464.5 eV, respectively. The area ratio of those two peaks is about 0.5, and the gap of the binding energy was 5.7 eV. Actually, some published results proved the titanium presence with an oxidation state lower than +4, such as Ti^{3+} and Ti^{2+} [26], which was not observed in this work. The binding energy of the Ti2p region decreases slightly (from 458.8 eV to 458.7 eV), while the binding energy of O1 s region increases slightly (from 530.1 eV to 530.2 eV). A new peak appears in the O1 s region after modification. These changes clearly show cyclodextrin linked to TiO_2 surface through the photo-induced self-assembly way. The reaction of β-CD linked to the TiO_2 surface is probably via Eq. (1) and Eq. (2) [10,12,27].

$$TiO_2 + h\nu \rightarrow e_{CB}^- + h_{VB}^+ \quad (1)$$

$$h_{VB}^+ + \beta\text{-CD} \rightarrow h_{CD}^+ \quad (2)$$

Fig. 3c and 3d show the high resolution XPS spectra of the O1 s region. The O1 s region of pure TiO_2 was decomposed into two contributions: the Ti–O bond in TiO_2 and the surface hydroxyl. After modification, the O1 s region has two organic contributions in addition to the inorganic oxygen species in pure TiO_2. Du et al. suggested that the formation of C=O double bonds is from an irreversible hole trap to an electron-hole recombination center [14]. They also suggested that cyclodextrin desorption is quite difficult to achieve even though a few transient C=C and C=O bonds are formed during the self-assembly process. The probability of desorption decreases roughly exponentially with the number of glucose units in the cyclodextrins. The FTIR and XPS data shown above sug-

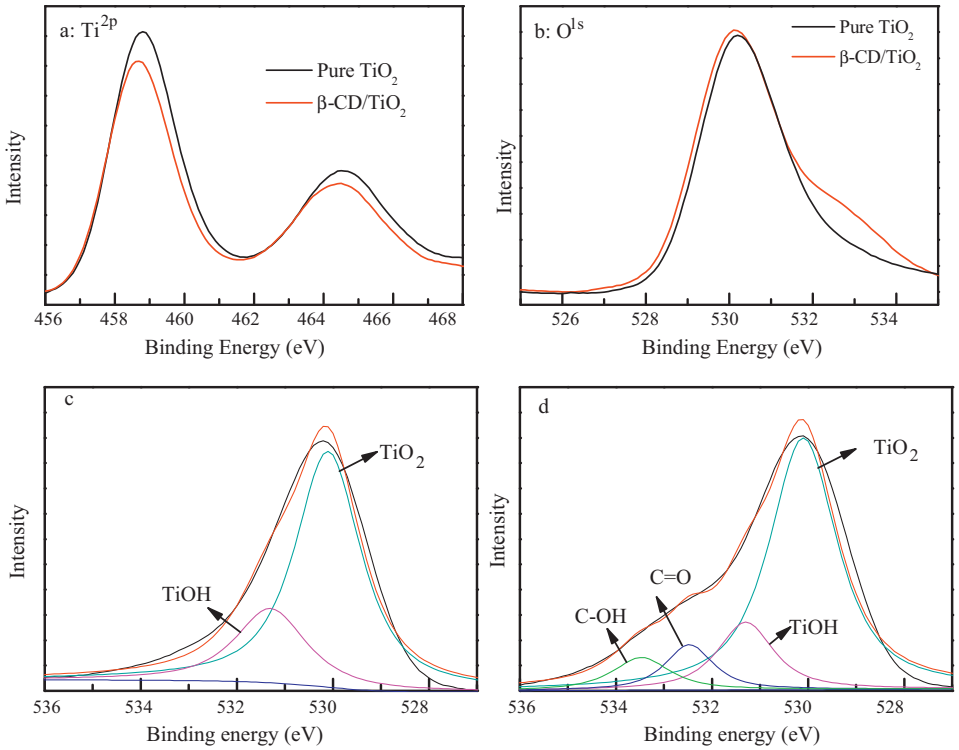

Fig. 3. XPS Spectra of Ti2p region (a), O1 s region (b), high resolution XPS spectra of O1 s region for pure TiO_2 (c) and TiO_2/β-CD hybrid powders (d).

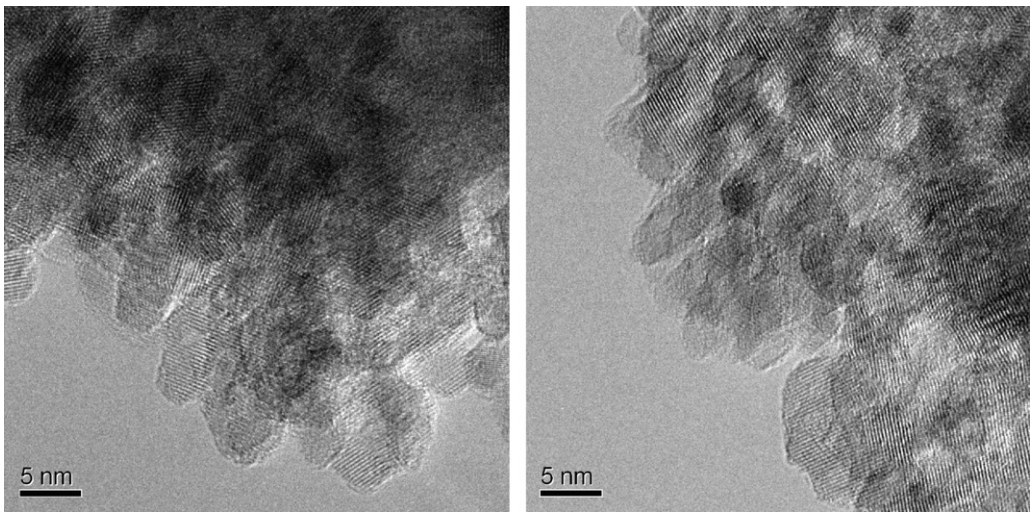

Fig. 4. HRTEM images of pure TiO_2 (left) and TiO_2/β-CD hybrid powders (right).

gest that the photogenerated holes are transferred to the linked cyclodextrin.

It was suggested that the holes' scavenging ability increases with the increasing number and spatial distribution of the hydroxyl groups in the polyhydroxyl compounds [27]. Therefore, β-CD could be highly reactive in capturing the photo generated holes. Du et al. also proposed that the positive charges carried by the holes transfer to those of the dissociated protons (H^+) resulting from the photoreaction of glucose unite in the adsorbed cyclodextrin. This hypothesis is quite reasonable because the pH value of the 1.0 g L^{-1} TiO_2/β-CD suspension is 5.5, which is noticeably less than 6.7 for the unmodified anatase TiO_2.

3.4. High Resolution Transmission Electron Microscopy (HRTEM)

HRTEM images were obtained on a JEOL JEM 2010FEF microscope operating at an accelerating voltage of 200 kV. As presented in Fig. 4 and Fig. S4 (Supporting Information), there was no change in the lattice structure of TiO_2 after β-CD modification. However, the outer boundary of the TiO_2/β-CD hybrid powder was distinctly different. From the solid TOC analysis of the TiO_2/β-CD hybrid nanoparticles, the final amount of linked β-CD on the TiO_2 surface was 9 μM/g.

3.5. Photocatalytic degradation of dye pollutants

Fig. 5 shows the dye removal percentage in the catalyst suspensions under λ ≥ 400 nm. The concentration of Orange II in the absence of catalyst under direct photolysis or in darkness in the presence of catalyst hardly changed. After 5 h of irradiation in the presence of anatase TiO_2, 36% of Orange II was decomposed. The removing efficiency of Orange II for Degussa P25 was 1.5 times that of anatase TiO_2, which was probably because the rutile crystallites in P25 may enhance the usage of visible light and slow the e^-/h^+ recombination. As expected, TiO_2/β-CD was the most efficient catalyst in Orange II degradation. After 5 h of irradiation, 93% of the Orange II was decomposed.

The photocatalytic performance of TiO_2/β-CD under different simulated irradiation sources was also studied. The performance of the catalyst compared to pure TiO_2 is shown in Fig. 6a. The TiO_2/β-CD hybrid powder effectively bleached dyes both under simulated solar conditions and visible light irradiation. After being modified by β-CD, the initial rate R_0 increased by 6.9, 2.6 and 1.9 times using a 420 nm filter, a 400 nm filter and simulated solar irradiation, respectively. The TOC of the solution disappeared rapidly whereas the TN decreased slightly. After 10 h irradiation at λ ≥ 420 nm, 0.662 mg/L of SO_4^{2-} was generated, which amounting 24% of the total sulfate in 10 mg/L Orange II. Because the results showed that the surface area and phase structure of TiO_2 was nearly identical before and after being modified by β-CD, the enhancement of the photocatalytic activity may be attributed to the enhancement of the electron transfer from the excited dye molecule to the TiO_2 conduction band. This will be discussed in a later section.

The degradation results carried out at pH 3.5 under room light clearly show that TiO_2/β-CD promotes electron injection from excited dyes to the TiO_2 conduction band (Fig. S5 and Fig. S6 of Supporting Information). The absorption intensity (200–600 nm) decreased due to the large adsorption of Orange II on the TiO_2 surface. The adsorption of Orange II was quite large at acidic pH and sharply decreased with a pH increase (Fig. S7 of Supporting Information). For TiO_2/β-CD, the absorption intensity also decreased in the first half hour. However, a new absorption peak at 250 nm appeared after one hour reaction, which means that photochemistry reactions occurred in addition to adsorption. After the reaction, the TiO_2 became red due to the adsorbed Orange II, while the color of the TiO_2/β-CD hybrid particle barely changed.

As shown in Fig. 7, the higher the initial Orange II concentration, the lower the degradation rate. These results are consistent with many studies in which activation by photon absorption was the first

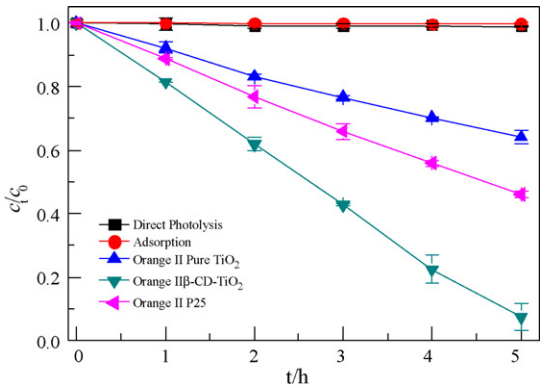

Fig. 5. Photocatalytic degradation of dyes aqueous solutions under various conditions. The initial concentration of Orange II and Rhodamine B was 10.0 and 5.0 mg L^{-1}, respectively. The concentration of catalyst was 1.0 g L^{-1}, the irrdiation source λ ≥ 400 nm.

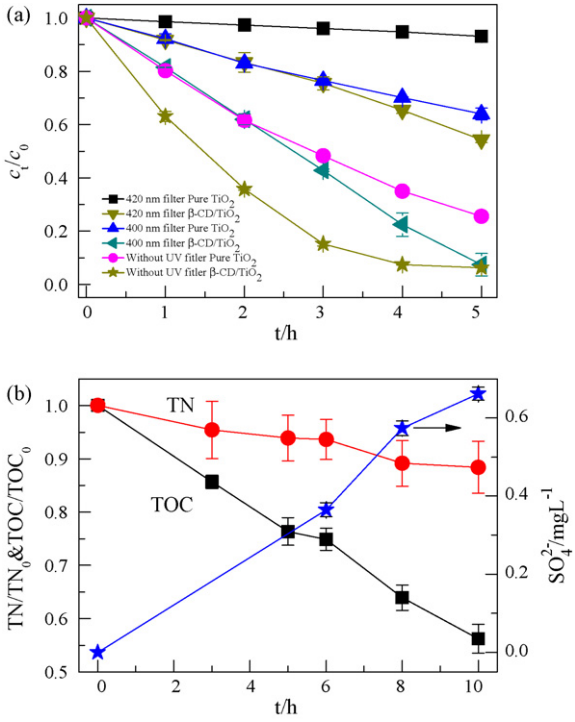

Fig. 6. Photocatalytic degradation of Orange II aqueous solutions under different irradiation source (a), changes of TOC, total nitrogen (TN) and SO_4^{2-} concentration as a function of irradiation time under $\lambda \geq 420$ nm (b). The initial concentration of Orange II was 10.0 mg L^{-1}. TiO_2/β-CD = 1.0 g L^{-1}.

reaction step and the reaction rates were reduced at higher initial concentrations. Furthermore, the amount of reactive species, like •OH, is determined by the light flux and the catalyst content in the dispersion.

The Langmuir–Hinshelwood kinetics rate model was applied to the heterogeneous degradation of many organic compounds [3,28,29]. The rate law is given by

$$R_0 = -\frac{dC}{dt} = \frac{k_{re}K_sC_0}{1 + K_sC_0}$$

where R_0 is the initial rate of disappearance of the substrate and C_0 is the initial concentration of Orange II. k_{re} is the reaction rate constant, and K_s is the Langmuir adsorption constant.

A non-linear regression fit of the Langmuir–Hinshelwood equation is shown in the inset of Fig. 7 indicating k_{re} = 2.76 mg L^{-1} h^{-1}.

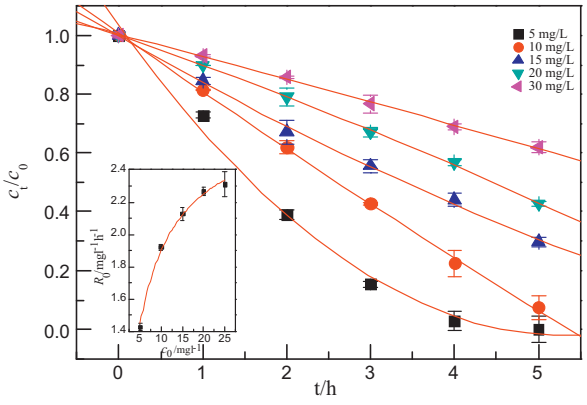

Fig. 7. The effect of Orange II initial concentration on the photocatalytic degradation under $\lambda \geq 400$ nm irradiation. The inset shows non-linear regression fit of the Langmuir–Hinshelwood equation. Orange II initial concentration various from 5.0 mg L^{-1} to 30 mg L^{-1}, TiO_2/β-CD = 1.0 g L^{-1}.

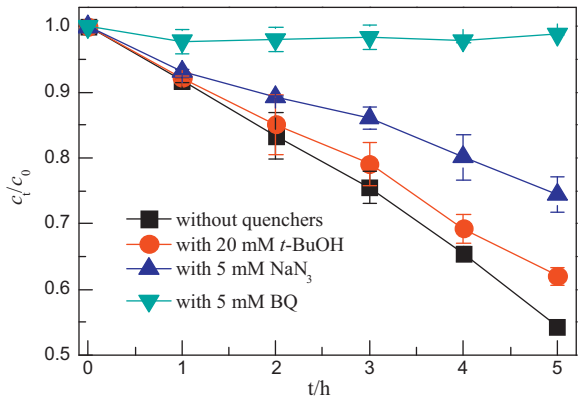

Fig. 8. Effects of scavengers on the photodegradation of Orange II under $\lambda \geq 420$ nm irradiation. Orange II = 10 mg L^{-1} TiO_2/β-CD = 1.0 g L^{-1}.

3.6. Mechanism study of the enhancement

Superoxide radicals, singlet oxygen, H_2O_2 and hydroxyl radicals are generally considered to be the oxidants in most dye photosensitized degradation on semiconductor surfaces [30–33]. To figure out the Orange II degradation mechanism, the influence of different scavengers on the degradation was investigated.

t-BuOH is generally used as a hydroxyl radical scavenger and the reaction constant of *t*-BuOH with hydroxyl radicals is 6.0×10^8 M^{-1} s^{-1} [34]. Excess *t*-BuOH (20 mM) was added to the solution to investigate the contribution of hydroxyl radical in this work. The results shown in Fig. 8 indicate that the degradation efficiency changes little in the presence of *t*-BuOH, which suggests that hydroxyl radicals do not play a major role in Orange II degradation

NaN_3 is a scavenger of singlet oxygen and can also react with hydroxyl radicals. The addition of 5 mM NaN_3 does not affect the degradation in the initial stages. The inhibition increases after 2 hours. Compared to the addition of *t*-BuOH, singlet oxygen was formed during the photochemistry reaction. It has been reported that singlet oxygen can be produced by the reaction of oxygen with the excited Orange II molecule [30].

BQ is used as a superoxide radical quencher in this study. Orange II degradation was completely suppressed with the addition of 5 mM BQ. The results prove that $\bullet O_2^-$ mediated oxidation pathways are dominant in Orange II degradation under visible irradiation.

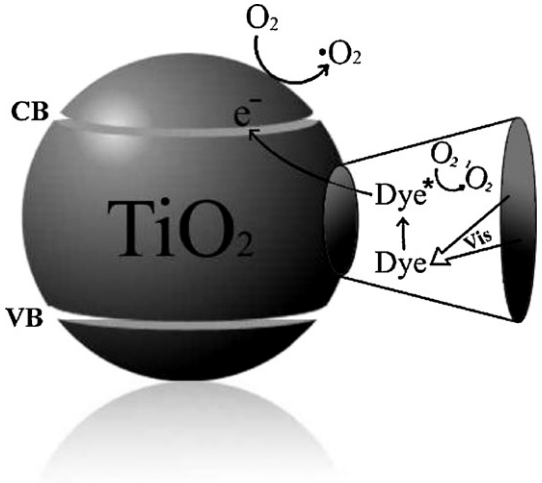

Fig. 9. Mode of photocatalytic degradation of dye pollutants over TiO_2/β-CD hybrid nanopowder under visible light irradiation.

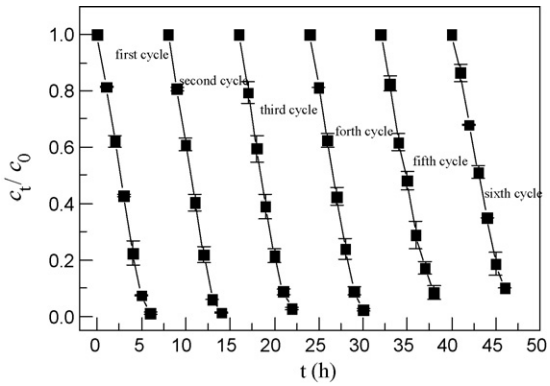

Fig. 10. Cyclic photocatalytic degradation of Orange II aqueous solution under $\lambda \geq 400$ nm irradiation: Orange II 10 mg L^{-1} each run.

Fig. 9 shows the possible pathways of dye degradation on TiO_2/β-CD. Dye molecules enter into the cavity of β-CD, which is linked to the TiO_2 surface in the equilibrium stage. An electron is rapidly injected from the excited dye to the conduction band [30–33]. The dye and dye cation radical then undergo degradation (Eq. vi–viii).

$$\text{Dye} + \text{TiO}_2/\beta\text{-CD} \rightarrow \text{TiO}_2/\beta\text{-CD}^{\bullet}\text{Dye} \quad \text{(i)}$$

$$\text{TiO}_2/\beta\text{-CD}^{\bullet}\text{Dye} + h\nu \rightarrow \text{TiO}_2/\beta\text{-CD}^{\bullet}{}^1\text{Dye}^* + \text{TiO}_2/\beta\text{-CD}^{\bullet}{}^3\text{Dye}^* \quad \text{(ii)}$$

$$\text{TiO}_2/\beta\text{-CD}^{\bullet}\text{Dye}^* \rightarrow (e)\text{TiO}_2/\beta\text{-CD} + \text{Dye}^{\bullet+} \quad \text{(iii)}$$

$$\text{TiO}_2/\beta\text{-CD}^{\bullet}\text{Dye}^* + \text{O}_2 \rightarrow \text{TiO}_2/\beta\text{-CD}^{\bullet}\text{Dye} + {}^1\text{O}_2 \quad \text{(iv)}$$

$$(e)\text{TiO}_2/\beta\text{-CD} + \text{O}_2 \rightarrow \text{TiO}_2/\beta\text{-CD} + \text{O}_2^{-} \quad \text{(v)}$$

$$\text{Dye}^{\bullet+} \rightarrow \text{Products} \quad \text{(vi)}$$

$$\text{Dye} + {}^1\text{O}_2 \rightarrow \text{Products} \quad \text{(vii)}$$

$$\text{Dye} + {}^{\bullet}\text{O}_2^{-} \rightarrow \text{Products} \quad \text{(viii)}$$

The sequential photodegradation experiments were performed to test the catalyst stability. As shown in Fig. 10, in the primary stage, 200 mL of 10 mg L^{-1} Orange II aqueous solution was completely decomposed after 6 h of irradiation. The decrease trend in the final degradation efficiency was 9% after 6 repetitive experiments.

Photogenerated radicals produce a great effect on the stability of the surface linked β-cyclodextrin. The reaction constant between β-CD and •OH is 4.2×10^9 L mol^{-1} s^{-1} [35]. However, the lifetime of •OH is quite short (about 20 ns) [36], and •OH is not the predominant radical under visible irradiation. Therefore, only those radicals generated in close proximity could react with β-CD. Because the TiO_2 surface is not fully covered with β-CD, it is quite reasonable to assume that the reaction between β-CD and •OH is limited. Another important radical in illumination of TiO_2/β-CD is the superoxide anion radical ($^{\bullet}O_2^-$). Actually, cyclodextrin derivates are used to improve the efficiency of $^{\bullet}O_2^-$ trapping using various nitrones as scavengers [37–39]. Therefore, the reaction between β-CD and diffusion mediated $^{\bullet}O_2^-$ can be neglected. In general, the lifetimes for the excited states of unreactive guests is prolonged when incorporated inside cyclodextrins. Therefore, cyclodextrin facilitates the electron injection from the excited dyes to the TiO_2 conduction band and thereby enhances the degradation.

4. Conclusion

TiO_2/β-CD hybrid nanoparticles were synthesized by a photo-induced self assembly process. The nanoparticles showed high reactivity for dye pollutant degradation under visible irradiation and simulated solar irradiation. The initial rate R_0 of Orange II disappearance increased by 6.9, 2.6 and 1.9 times using a 420 nm filter, a 400 nm filter and simulated solar irradiation, respectively. $^{\bullet}O_2^-$ mediated oxidation pathways are dominant for Orange II degradation under visible irradiation. The reaction between β-CD and diffusion mediated $^{\bullet}O_2^-$ was negligible, which makes TiO_2/β-CD an effective and stable catalyst. β-CD could increase the excited states lifetimes of unreactive guests and facilitate electron transfer from the excited dye to TiO_2 conduction band, which enhances dye pollutant degradation.

Acknowledgements

The author Xu Zhang thanks Dr. Huayi Yin for BET analysis and Miss Bo Feng for helpful technical discussions regarding the mechanism. This work was financed by the Natural Science Foundation of P.R. of China (No. 20777057) and Young Scholar of Distinction of Ministry of Education.

Appendix A. Supplementary data

Supplementary data associated with this article can be found, in the online version, at doi:10.1016/j.jhazmat.2010.09.005.

References

[1] A. Fujishima, K. Honda, Electrochemical Photolysis of Water at a Semiconductor Electrode, Nature 238 (1972) 37–38.
[2] S.T. Martin, H. Herrmann, W. Choi, M.R. Hoffmann, Time-Resolved Microwave Conductivity Part 1. TiO_2 Photoactivity and Size Quantization, J. Chem. Soc. Faraday Trans. 90 (1994) 3315–3322.
[3] M.R. Hoffmann, S.T. Martin, W. Choi, D.W. Bahnemann, Environmental Applications of Semiconductor Photocatalysis, Chem. Rev. 95 (1995) 69–96.
[4] A. Fujishima, T.N. Rao, D.A. Tryk, Titanium dioxide photocatalysis, J. Photochem. Photobiol. C: Photochem. Rev. 1 (2000) 1–21.
[5] K. Kabra, R. Chaudhary, R.L. Sawhney, Treatment of Hazardous Organic and Inorganic Compounds through Aqueous-Phase Photocatalysis: A Review, Ind. Eng. Chem. Res. 43 (2004) 7683–7696.
[6] E. Forgacs, T. Cserháti, G. Oros, Removal of synthetic dyes from wastewaters: a review, Environ. Int. 30 (2004) 953–971.
[7] I. Willner, Y. Eichen, Titanium dioxide and cadmium sulfide colloids stabilized by β-cyclodextrins: tailored semiconductor-receptor systems as a means to control interfacial electron-transfer processes, J. Am. Chem. Soc. 109 (1987) 6862–6863.
[8] I. Willner, Y. Eichen, A.J. Frank, Tailored Semiconductor-Receptor Colloids: Improved Photosensitized H2 Evolution from Water with TiO_2-β-Cyclodextrin Colloids, J. Am. Chem. Soc. 111 (1989) 1884–1886.
[9] I. Willner, Y. Eichen, B. Willner, Supermolecular semiconductor receptor assemblies: improved electron transfer at TiO_2-β-cyclodextrin colloids interfaces, Res. Chem. Intermed. 20 (1994) 681–700.
[10] T. Tachikawa, S. Tojo, M. Fujitsuka, T. Majima, One-Electron Oxidation Pathways during β-Cyclodextrin-Modified TiO_2 Photocatalytic Reactions, Chem. Eur. J. 12 (2006) 7585–7594.
[11] N.M. Dimitrijevic, Z.V. Saponjic, D.M. Bartels, M.C. Thurnauer, D.M. Tiede, T. Rajh, Revealing the Nature of Trapping Sites in Nanocrystalline Titanium Dioxide by Selective Surface Modification, J. Phys. Chem. B 107 (2003) 7368–7375.
[12] N.M. Dimitrijevic, T. Rajh, Z.V. Saponjic, L. de la Garza, D.M. Tiede, Light-Induced Charge Separation and Redox Chemistry at the Surface of TiO_2/Host-Guest Hybrid Nanoparticles, J. Phys. Chem. B 108 (2004) 9105–9110.
[13] J. Feng, A. Miedaner, P. Ahrenkiel, M.E. Himmel, C. Curtis, D. Ginley, Self-Assembly of Photoactive TiO_2-Cyclodextrin Wires, J. Am. Chem. Soc. 127 (2005) 14967–14968.
[14] M. Du, J. Feng, S.B. Zhang, Photo-Oxidation of Polyhydroxyl Molecules on TiO_2 Surfaces: From Hole Scavenging to Light-Induced Self-Assembly of TiO_2-Cyclodextrin Wires, Phys. Rew. Lett. 98 (2007), pp. 066102-1-166102-4.
[15] S. Anandan, M. Yoon, Photocatalytic degradation of Nile red using TiO_2-β cyclodextrin colloids, Catal. Commun. 5 (2004) 271–275.
[16] P. Lu, F. Wu, N.S. Deng, Enhancement of TiO_2 photocatalytic redox ability by β-cyclodextrin in suspended solutions, Appl. Catal. B: Environ. 53 (2004) 87–93.

[17] G.H. Wang, F. Wu, X. Zhang, M.D. Luo, N.S. Deng, Enhanced TiO_2 photocatalytic degradation of bisphenol A by β-cyclodextrin in suspended solutions, J. Photochem Photobio A: Chem. 179 (2006) 49–56.
[18] X. Zhang, F. Wu, Z. Wang, Y. Guo, N.S. Deng, Photocatalytic degradation of 4, 4′-biphenol in TiO_2 suspension in the presence of cyclodextrins: A trinity integrated mechanism, J. Mol. Catal. A-Chem. 301 (2009) 134–139.
[19] S.H. Toma, J.A. Bonacin, K. Araki, H.E. Toma, Selective host–guest interactions on mesoporous TiO_2 films modified with carboxymethyl-β-cyclodextrin, Surf. Sci. 600 (2006) 4591–4597.
[20] W. Zhou, K. Pan, L.L. Zhang, C.G. Tian, H.G. Fu, Solar-induced self-assembly of TiO_2–β-cyclodextrin–MWCNT composite wires, Phys. Chem. Chem. Phys. 11 (2009) 1713–1718.
[21] M. Montalti, A. Credi, L. Prodi, T. Gandolfi, Handbook of Photochemistry, third ed., Marcel Dekker, New York, 2006.
[22] X. Zhang, F. Wu, N.S. Deng, Degradation of paracetamol in self assembly β-cyclodextrin/TiO_2 suspension under visible irradiation, Catal. Commun. 11 (2010) 422–425.
[23] J.S. Fritz, G.H. Shenk, Quantitative Analytical Chemistry, Allyn & Bacon inc, Boston, 1974.
[24] Z.C. Orel, M.K. Gunde, B. Orel, Application of the Kubelka-Munk theory for the determination of the optical properties of solar absorbing paints, Prog. Org. Coat. 30 (1997) 59–66.
[25] T. Rajh, L.X. Chen, K. Lukas, T. Liu, M.C. Thurnauer, D.M. Tiede, Surface Restructuring of Nanoparticles: An Efficient Route for Ligand-Metal Oxide Crosstalk, J. Phys. Chem. B 106 (2002) 10543–10552.
[26] W.J. Zhang, Y. Li, S.L. Zhu, Surface modification of TiO_2 film by iron doping using reactive magnetron sputtering, Chem. Phys. Lett. 373 (2003) 333–337.
[27] I.A. Shkrob, M.C. Sauer Jr., D. Gosztola, Efficient, Rapid Photooxidation of Chemisorbed Polyhydroxyl Alcohols and Carbohydrates by TiO_2 Nanoparticles in an Aqueous Solution, J. Phys. Chem. B 108 (2004) 12512–12517.
[28] C.S. Turchi, D.F. Ollis, Photocatalytic degradation of organic water contaminants: Mechanisms involving hydroxyl radical attack, J. Catal. 122 (1990) 178–192.
[29] B. Jenny, P. Pichat, Determination of the actual photocatalytic rate of hydrogen peroxide decomposition over suspended titania. Fitting to the Langmuir–Hinshelwood form, Langmuir 7 (1991) 947–954.
[30] M. Stylidi, D.I. Kondarides, X.E. Verykios, Visible light-induced photocatalytic degradation of Acid Orange 7 in aqueous TiO_2 suspensions, Appl. Catal. B: Environ. 47 (2004) 189–201.
[31] K. Vinodgopal, D.E. Wynkoop, P.V. Kamat, Environmental Photochemistry on Semiconductor Surfaces: Photosensitized Degradation of a Textile Azo Dye, Acid Orange 7, on TiO_2 Particles Using Visible Light, Environ. Sci. Technol. 30 (1996) 1660–1666.
[32] C. Nasr, K. Vinodgopal, L. Fisher, S. Hotchandani, A.K. Chattopadhyay, P.V. Kamat, Environmental Photochemistry on Semiconductor Surfaces. Visible Light Induced Degradation of a Textile Diazo Dye, Naphthol Blue Black, on TiO_2 Nanoparticles, J. Phys. Chem. 100 (1996) 8436–8442.
[33] T.X. Wu, G.M. Liu, J.C. Zhao, H. Hidaka, N. Serpone, Evidence for H_2O_2 generation during the TiO_2-Assisted Photodegradation of Dyes in Aqueous Solutions under visible Light Illumination, J. Phys. Chem. B 103 (1999) 4862–4867.
[34] L.H. Chia, X.M. Tang, L.K. Weavers, Kinetics and Mechanism of Photoactivated Periodate Reaction with 4-Chlorophenol in Acidic Solution, Environ. Sci. Technol. 38 (2004) 6875–6880.
[35] O. Hayaishi, E. Niki, M. Kondo, T. Yoshikawa, Medical Biochemical and Chemical Aspects of Free Radicals, Elsevier, Amsterdam, 1989.
[36] M.A. Grela, M.E.J. Coronel, A.J. Colussi, Quantitative Spin-Trapping Studies of Weakly Illuminated Titanium Dioxide Sols. Implications for the Mechanism of Photocatalysis, J. Phys. Chem. 100 (1996) 16940–16946.
[37] H. Karoui, A. Rockenbauer, S. Pietria, P. Tordo, Spin trapping of superoxide in the presence of β-cyclodextrins, Chem. Commun. 38 (2002) 3030–3031.
[38] Y.B. Han, B. Tuccio, R. Lauricella, F.A. Villamena, Improved Spin Trapping Properties by β-Cyclodextrin – Cyclic Nitrone Conjugate, J. Org. Chem. 73 (2008) 7108–7117.
[39] D. Bardelang, L. Charles, J. Finet, L. Jicsinszky, H. Karoui, S.R.A. Marque, V. Monnier, A. Rockenbauer, R. Rosas, P. Tordo, α-Phenyl-N-tert-butylnitrone-Type Derivatives Bound to β-Cyclodextrins: Syntheses, Thermokinetics of Self-Inclusion and Application to Superoxide Spin-Trapping, Chem. Eur. J. 13 (2007) 9344–9354.